2023 14th International Conference on Information and Communication Technology Convergence (ICTC) | 979-8-3503-1327-7/23/$31.00 ©2023 IEEE | DOI: 10.1109/ICTC58733.2023.10392383

Hybrid Relay and OIRS-Aided Free Space Optical Communication System with Distributed Computing

*

1st Haibo Wang
National Mobile Communications Research Laboratory
Southeast University
Nanjing, China
haibowang@seu.edu.cn

2nd Zaichen Zhang
National Mobile Communications Research Laboratory
Southeast University
Nanjing, China
zczhang@seu.edu.cn

3rd Yingmeng Ge
National Mobile Communications Research Laboratory
Southeast University
Nanjing, China
230208082@seu.edu.cn

4th Baiping Xiong
National Mobile Communications Research Laboratory
Southeast University
Nanjing, China
xiongbp@seu.edu.cn

***Abstract*—In order to simultaneously solve the problems of beam diffusion and occlusion in long-distance free space optics (FSO) transmission, a hybrid relay and OIRS-aided FSO communication system with distributed computing is proposed in this paper. In the front-end link, the base station sends optical signals to the optical relay. The signal is forwarded to the OIRS after being collimated and amplified by the optical relay, and then transmitted to the user after being reflected by the OIRS. we derive closed-form solutions of the system's precise outage probability, asymptotic outage probability and BER by jointly considering optical relay gain, OIRS physical model, pointing error, atmospheric turbulence, atmospheric absorption, etc. Based on theoretical analysis and simulation results, the system's parameter settings have been discussed.**

***Index Terms*—optical intelligent reflecting surface, free space optics, optical channel modeling, asymptotic analysis.**

I. Introduction

With the continuous improvement of communication capacity requirements and frequency bands, optical wireless communication technology has gradually become an important research direction of future wireless communication systems, which has attracted widespread attention. Optical wireless communication, especially free space optics (FSO) communication technology based on wireless laser communication, has the advantages of high speed, high capacity, rich spectrum resources and high confidentiality [1]–[3]. Therefore, for future broadband wireless communication, FSO communication is a promising and important research direction. However, due to the diffusion angle and high directivity of the optical signal, the diffusion and easy blocking of the optical signal become an important factor restricting the system's performance in the long-distance FSO transmission. Under the existing technology, the diffusion of optical signals can be solved by optical relay [4]–[6]. By setting up optical relay nodes in free space, the system can re-collimate optical signals, thereby reducing the diffusion angle of optical signals in long-distance transmission. The defect that optical signals are easily blocked has been solved for a long time by avoiding scenes with obstacles, such as using FSO systems for high-altitude communication, which seriously restricts the application scenarios of FSO systems.

Optical intelligent reflecting surface (OIRS), as a new type of programmable communication device, can perform operations such as reflection, shaping, and beam splitting on light beams, which is expected to solve the problem that optical signals are easily blocked [7], [8]. By setting one or more OIRSs in the environment, the optical signal is reflected by the OIRS to reach the user, thereby bypassing obstacles on the direct path. When an OIRS path is blocked, the base station can select an unblocked OIRS for signal transmission, thereby improving the robustness of the system [9], [10].

In order to simultaneously solve the problems of beam diffusion and occlusion in long-distance FSO transmission, a hybrid relay and OIRS-aided distributed FSO system is proposed in this paper. In the front-end link, the base station sends optical signals to the optical relay. The signal is forwarded to the OIRS after being collimated and amplified by the optical relay, and then transmitted to the user after being reflected by the OIRS. Different from the existing broadband radio frequency communication system, this system uses optical carrier as the communication medium, which has extremely high communication bandwidth and speed [11]–[13]. Through

This work is supported by the NationalKey R&D Program of China (2018YFB1801101, 2020YFB1806603), NSFC projects (61960206005, 61803211, 61971136, and 62171127), the Fundamental Research Funds for the Central Universities (2242022k30001), and Research Fund of National Mobile Communications Research Laboratory. Zaichen Zhang is the corresponding author.

the OIRS in the space, the system adopts the distributed computing method to solve many defects of the long-distance FSO system, so it has certain advantages compared with the traditional broadband wireless communication. Different from the existing OIRS-aided FSO system, this paper also conducts mathematical modeling and derivation for the optical relay and OIRS in the system, and obtains the closed-form expression of the performance of the hybrid relay and OIRS-aided distributed FSO system [14]–[16]. At the same time, when conducting channel modeling and performance analysis, this paper comprehensively considers the factors in the actual system such as optical relay gain, OIRS physical model, pointing error, atmospheric turbulence, and path loss, which fits the actual system.

The contributions of this paper are as follows:

1. We design a hybrid relay and OIRS-aided distributed FSO system, and perform mathematical modeling on it.

2. We derive closed-form solutions of the system's precise outage probability, asymptotic outage probability and BER by jointly considering optical relay gain, OIRS physical model, pointing error, atmospheric turbulence, atmospheric absorption, etc.

3. Based on theoretical analysis and simulation results, we have discussed the system's parameter settings.

The rest of this paper are organized as follows. Section II introduces our system model and derives the expressions of the signals at the user. In Section III, we deduce the channel fading correlation expressions of the two links from the base station to the relay and from the relay to the user respectively. In Section IV, we derive the expression for system's precise outage probability, asymptotic outage probability and BER. Section V shows some numerical results and makes some discussions on system parameters. Section VI draws conclusion.

II. System Model

In this paper, we consider a hybrid relay and OIRS-aided distributed FSO system, as shown in Fig. 1. In the front-end link between the base station and the relay, we use the FSO communication based on the direct path for long-distance high-speed data transmission. The front-end link is mainly suitable for the construction of communication links between base stations and large facilities such as buildings, trains, and subways. Since the communication link is located in an area that is not easily disturbed, such as high altitude, it can be set based on the direct path. In the back-end link between the relay and the user, we use one or more OIRS to assist the FSO communication, so as to build multiple artificially controlled optical channels. When the direct channel between the relay and the user is blocked or the channel condition is poor, the optical signal can be reflected to the user through the OIRS, thereby improving the overall robustness of the system. The relay can even choose among multiple OIRS, and select the OIRS with the best channel condition for transmission. At the same time, since OIRS are set in various positions in free space, each OIRS can be responsible for users in a space area, thus realizing a distributed FSO system.

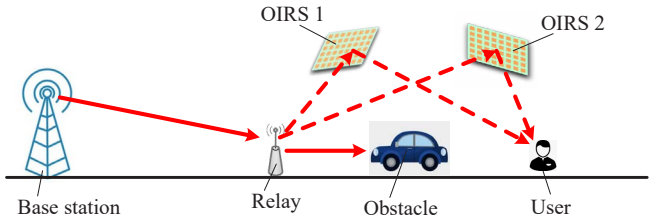

Fig. 1: Schematic diagram of a hybrid relay and OIRS-aided distributed FSO system.

Assuming that the system consists of a base station, a relay, I OIRSs and J users. Then the signal received at the relay y_r can be expressed as

$$y_r = h_{s,r} s_t + n_r, \tag{1}$$

where $h_{s,r}$ is the channel fading from the source to the relay; Since we utilize IM/DD with OOK modulation in this system, $s_t = 0$ or $2P_t$, where P_t is the average optical transmitted power at the base station; n_r is the zero-mean Gaussian white noise from the relay with a variance of $\sigma_{n_r}^2$. Then the signal received by the user j can be expressed as

$$\begin{aligned} y_{u_j} &= \rho_j \sum_{i=1}^{I} \beta_i h_{r,o_i} h_{o_i,u_j} \alpha_i g_r y_r + n_{u_j} \\ &= \rho_j \sum_{i=1}^{I} \beta_i h_{r,o_i} h_{o_i,u_j} \alpha_i g_r h_{s,r} s_t \\ &+ \rho_j \sum_{i=1}^{I} \beta_i h_{r,o_i} h_{o_i,u_j} \alpha_i g_r n_r + n_{u_j}, \end{aligned} \tag{2}$$

where ρ_j is the power allocation coefficient for user j and $\sum_{j=1}^{J} \rho_j = 1$; β_i indicates whether the OIRS i is selected, $\beta_i = 0$ or 1 and $\sum_{i=1}^{I} \beta_i = 1$; h_{r,o_i} is the channel fading from the relay to the OIRS i; h_{o_i,u_j} is the channel fading from the OIRS i to the user j; α_i is the attenuation coefficient from the OIRS i; g_r is the optical signal gain of the relay; n_{u_j} is the zero-mean Gaussian white noise from the user j with a variance of $\sigma_{n_{u_j}}^2$.

III. Channel Model

A. Channel Fading from Base Station to Relay

Below we will analyze the channel fading from the base station to the relay, which arises from pointing error, atmospheric turbulence and path loss. Therefore, the channel fading from the source to the relay $h_{s,r}$ can be expressed as

$$h_{s,r} = h_{p_{s,r}} h_{a_{s,r}} h_{l_{s,r}}, \tag{3}$$

where $h_{p_{s,r}}$ is the channel fading from the source to the relay caused by pointing error, $h_{a_{s,r}}$ is the channel fading from the source via OIRS i to the relay caused by atmospheric turbulence, and $h_{l_{s,r}}$ is the channel fading from the source via OIRS i to the relay caused by path loss.

1) Pointing Error: In the FSO system, due to the narrow beam and high directivity, the offset of the light spot at the receiver relative to the center of the receiver will cause a certain signal fading, which is caused by the jitter of the transmitter and the propagation of the beam in free space and is called pointing error. According to [2], [3], the probability density function of the channel fading caused by pointing error $h_{p_{s,r}}$ in the FSO link can be expressed as

$$f_{h_{p_{s,r}}}(h_{p_{s,r}}) = \frac{\omega_{zeq}^2}{4A_0\sigma_{\theta_t}^2 l_{s,r}^2} \times \left(\frac{h_{p_{s,r}}}{A_0}\right)^{\frac{\omega_{zeq}^2}{4A_0\sigma_{\theta_t}^2 l_{s,r}^2}-1}, \quad (4)$$

where A_0 is the fraction of the receiver's collected power at $R_r = 0$ and ω_{zeq} is the equivalent beam width. We have $A_0 = [\mathrm{erf}(z)]^2$ and $\omega_{zeq}^2 = \omega_z^2 \frac{\sqrt{\pi}\mathrm{erf}(z)}{2zexp(-z^2)}$, where $z = \sqrt{\frac{\pi}{2}}\frac{a}{\omega_z}$ is the ratio between aperture radius and the beam width, $\mathrm{erf}(x) = \frac{2}{\sqrt{\pi}}\int_0^x e^{-t^2}dt$ is the error function, ω_z is the beam waist radius and can be approximated by $\omega_z = \phi_t l_{s,r}$, ϕ_t is the divergence angle of the beam at the transmitter.

2) Atmospheric Turbulence: Due to the long length of the FSO link in this system, the fading caused by atmospheric turbulence is an important factor that cannot be ignored. At the same time, since the OIRS is set near the ground, the whole system should be set in the area near the ground, which fits the weak turbulence model [2], [3]. Therefore, in this system, we choose the weak turbulence model of atmospheric turbulence for analysis. For weak turbulence, the intensity fluctuation is modeled as a log-normal distribution, which is experimentally verified. According to [2], [3], the PDF of the channel fading caused by atmospheric turbulence $h_{a_{s,r}}$ can be expressed as

$$f_{h_{a_{s,r}}}(h_{a_{s,r}}) = \frac{1}{2h_{a_{s,r}}\sqrt{2\pi\sigma_X^2}} e^{\frac{\left(lnh_{a_{s,r}}+2\sigma_X^2\right)^2}{8\sigma_X^2}} \quad (5)$$

where σ_X^2 is the log-amplitude variance, which is given by

$$\sigma_X^2 = 0.30545\kappa^{\frac{7}{6}} C_n^2(L) l_{s,r}^{\frac{11}{6}} \approx \frac{\sigma_R^2}{4} \quad (6)$$

where $C_n^2(L)$ is the index of refraction structure parameter at altitude L, which can be assumed to be constant along the propagation path, $\kappa = \frac{2\pi}{\lambda}$ is the optical wavenumber, λ is the optical wavelength, and σ_R^2 is the Rytov variance defined as

$$\sigma_R^2 = 1.23 C_n^2 \kappa^{\frac{7}{6}} l_{s,r}^{\frac{11}{6}} \quad (7)$$

3) Path Loss: For FSO links, the path loss of the signal mainly comes from atmospheric absorption, which is affected mainly by wavelength, link length, and weather conditions. In this system, we choose light source with a wavelength of 1550 nm, which is widely used in the FSO link due to its low absorption rate in the atmosphere [17], [18]. According to [18], the path loss at 1550 nm can be expressed as

$$h_{l_{s,r}} = 10^{-\frac{\mu_{s,r}}{l_{s,r}}10^4}, \quad (8)$$

where $\mu_{s,r}$ represents the atmospheric absorption coefficient per km in the optical channel under current weather conditions, whose unit is dB/km. Since the transition rate of weather conditions is much slower than the signal transmission rate, the channel fading caused by path loss can be regarded as large-scale fading.

4) Channel Fading of the Front-end Link: Since $h_{l_{s,r}}$ can be modeled as a large-scale fading, the PDF of channel fading from the source to the relay $h_{s,r}$ can be expressed as

$$\begin{aligned} &f_{h_{s,r}}(h_{s,r}) \\ &= \int f_{h_{s,r}|h_{a_{s,r}}}\left(h_{s,r} \mid h_{a_{s,r}}\right) f_{h_{a_{s,r}}}\left(h_{a_{s,r}}\right) dh_{a_{s,r}} \end{aligned} \quad (9)$$

where $f_{h_{s,r}|h_{a_{s,r}}}\left(h_{s,r} \mid h_{a_{s,r}}\right)$ is the conditional PDF given the channel fading of atmospheric turbulence $h_{a_{s,r}}$, which can be derived from (3) and (13) as

$$\begin{aligned} f_{h_{s,r}|h_{a_{s,r}}}\left(h_{s,r} \mid h_{a_{s,r}}\right) &= \frac{1}{h_{a_{s,r}}h_{l_{s,r}}} f_{h_{p_{s,r}}}\left(\frac{h_{s,r}}{h_{a_{s,r}}h_{p_{s,r}}}\right) \\ &= \frac{10^{\frac{\mu_{s,r}l_{s,r}}{10^4}}\varepsilon_{s,r}}{h_{a_{s,r}}A_0}\left(\frac{h_{s,r}10^{\frac{l_{s,r}}{10^4}}}{h_{a_{s,r}}A_0}\right)^{\varepsilon_{s,r}-1}, \end{aligned} \quad (10)$$

where $\varepsilon_{s,r} = \frac{\omega_{zeq}^2}{4A_0\sigma_{\theta_t}^2 l_{s,r}^2}$.

Substituting (10) and (5) into (9), we can obtain the closed-form PDF of $h_{s,r}$ as (11)

B. Channel Fading from Relay to User

Since in this system, the channel between the relay and the user is still an FSO channel, the factors affecting the channel fading between the relay and the user are still pointing error, atmospheric turbulence and path loss. However, unlike the front-end link, there is an OIRS between the relay and the user to reflect the light beam, which affects the channel fading in the system. For channel fading caused by atmospheric turbulence and path loss, the influence of OIRS reflection is mainly on the extension of the channel path, which does not change the channel fading distribution. As for the pointing error, the reflection of the OIRS will increase the jitter of the beam at the transmitting end and at the same time introduce the jitter of the OIRS plane, which will change the channel fading distribution caused by the pointing error. According to [10], [15], [16], we can obtain the PDF of the pointing error angle at the relay's receiving plane θ_r as

$$\begin{aligned} f_{\theta_r}(\theta_r) =& \frac{\theta_r}{\left(1+\frac{l_{r,o_i}}{l_{o_i,u_j}}\right)^2\sigma_{\theta_r'}^2 + 4\sigma_{\beta_i}^2} \\ &\times exp\left(-\frac{\theta_r^2}{2\left(1+\frac{l_{r,o_i}}{l_{o_i,u_j}}\right)^2\sigma_{\theta_r'}^2 + 8\sigma_{\beta_i}^2}\right), \end{aligned} \quad (12)$$

where $\theta_r^{'}$ is the beam's jitter angle at the relay while pointing to OIRS i; β_i is the jitter angle of OIRS, which is independent of the relay; $\sigma_{\theta_r'}^2$ is the variance of θ_r; $\sigma_{\beta_i}^2$ is the variance of β_i; l_{r,o_i} is the distance from the relay to the OIRS i; l_{o_i,u_j} is the distance from the OIRS i to the user j. According to [15],

$$
\begin{aligned}
f_{h_{s,r}}(h_{s,r}) &= \frac{10^{\frac{\varepsilon_{s,r}\mu_{s,r}l_{s,r}}{10^4}}\varepsilon_{s,r}}{A_0^{\varepsilon_{s,r}}} h_{s,r}^{\varepsilon_{s,r}-1} \times \int_{\frac{10^{\frac{\mu_{s,r}l_{s,r}}{10^4}}h_{s,r}}{A_0}}^{\infty} h_{a_{s,r}}^{-\varepsilon_{s,r}} f_{h_{a_{s,r}}}\left(h_{a_{s,r}}\right) dh_{a_{s,r}} \\
&= \frac{10^{\frac{\varepsilon_{s,r}\mu_{s,r}l_{s,r}}{10^4}}\varepsilon_{s,r}}{A_0^{\varepsilon_{s,r}}} h_{s,r}^{\varepsilon_{s,r}-1} \times \int_{\frac{10^{\frac{\mu_{s,r}l_{s,r}}{10^4}}h_{s,r}}{A_0}}^{\infty} h_{a_{s,r}}^{-\varepsilon_{s,r}} \frac{1}{2h_{a_{s,r}}\sqrt{2\pi\sigma_X^2}} \times exp\left(\frac{\left(lnh_{a_{s,r}} + 2\sigma_X^2\right)^2}{8\sigma_X^2}\right) dh_{a_{s,r}} \\
&= \frac{10^{\frac{\varepsilon_{s,r}\mu_{s,r}l_{s,r}}{10^4}}\varepsilon_{s,r}}{2A_0^{\varepsilon_{s,r}}} h_{s,r}^{\varepsilon_{s,r}-1} e^{2\sigma_X^2\varepsilon_{s,r}(1+\varepsilon_{s,r})} \times erfc\left(\frac{ln\frac{h_{s,r}10^{\frac{\mu_{s,r}l_{s,r}}{10^4}}}{A_0} + 2\sigma_X^2 + 4\varepsilon_{s,r}\sigma_X^2}{2\sqrt{2}\sigma_X}\right).
\end{aligned} \tag{11}
$$

[16], the PDF of the channel fading caused by pointing error in the backend link $h_{p_{r,u_j}}$ can be derived as

$$
\begin{aligned}
f_{h_{p_{r,u_j}}}(h_{p_{r,u_j}}) &= \frac{\omega_{zeq}^{2'}}{4A_0\sigma_{\theta_r'}^2\left(l_{r,o_i}+l_{o_i,u_j}\right)^2 + 16A_0\sigma_{\beta_i}^2 l_{r,o_i}^2} \\
&\times \left(\frac{h_{p_{r,u_j}}}{A_0}\right)^{\frac{\omega_{zeq}^{2'}}{4\sigma_{\theta_r'}^2\left(l_{r,o_i}+l_{o_i,u_j}\right)^2+16\sigma_{\beta_i}^2 l_{r,o_i}^2}-1}.
\end{aligned} \tag{13}
$$

IV. Performance Analysis

A. Outage Probability

Since this system is a dual-link cascaded communication system, we use decode and forward (DF) method at the relay to ensure the accuracy of signal transmission. Then the outage probability of the user j 's received signal can be expressed as

$$
\begin{aligned}
P_{out}(\gamma_{th}) &= 1 - (1 - F_{\gamma_{s,r}}(\gamma_{th}))(1 - F_{\gamma_{r,u_j}}(\gamma_{th})) \\
&= F_{\gamma_{s,r}}(\gamma_{th}) + F_{\gamma_{r,u_j}}(\gamma_{th}) - F_{\gamma_{s,r}}(\gamma_{th})F_{\gamma_{r,u_j}}(\gamma_{th}),
\end{aligned} \tag{14}
$$

which indicates that the communication system is not interrupted only when neither the front-end link nor the back-end link is interrupted, where $F_{\gamma_{s,r}}(\gamma_{th})$ is the cumulative distribution function (CDF) of the front-end channel's signal-to-noise ratio (SNR) from the source to the relay, $F_{\gamma_{r,u_j}}(\gamma_{th})$ is the CDF of the back-end channel's SNR from the relay to the user j, and γ_{th} is the outage threshold of SNR.

1) Front-end Link: According to (1), the instantaneous SNR from the source to the relay $\gamma_{s,r}$ can be presented as

$$
\gamma_{s,r} = \frac{2h_{s,r}^2 P_t^2}{\sigma_{n_r}^2}. \tag{15}
$$

Substituting (15) into (11), we can derive the CDF of $\gamma_{s,r}$ as

$$
\begin{aligned}
F_{\gamma_{s,r}}(\gamma_{th}) &= \frac{1}{2} exp\left(\varepsilon_{s,r}\chi_{s,r} + 2\varepsilon_{s,r}\sigma_X^2 + 2\varepsilon_{s,r}^2\sigma_X^2\right) \\
&\times erfc\left(\frac{\chi_{s,r} + 2\sigma_X^2 + 4\varepsilon_{s,r}\sigma_X^2}{\sqrt{8}\sigma_X}\right) \\
&- \frac{1}{2} erfc\left(\frac{\chi_{s,r} + 2\sigma_X^2}{\sqrt{8}\sigma_X}\right),
\end{aligned} \tag{16}
$$

where $\chi_{s,r} = \frac{1}{2}ln\frac{\gamma_{th}}{2} + ln\frac{\sigma_{n_r}}{A_0 P_t h_{l_{s,r}}}$.

2) Back-end Link: According to (2), the instantaneous SNR of the user j γ_{r,u_j} can be presented as

$$
\gamma_{r,u_j} = \frac{2\sum_{i=1}^{N}\beta_i^2\alpha_i^2 h_{r,o_i}^2 h_{o_i,u_j}^2 g_r P_t^2}{\sigma_{n_{u_j}}^2}. \tag{17}
$$

In this system, we adopt the strategy of selecting the optimal OIRS, namely $\beta_i = 0$ or 1, $\sum_{i=1}^{I}\beta_i = 1$. Assuming that the optimal OIRS we choose is OIRS k, γ_{r,u_j} can be expressed as

$$
\gamma_{r,u_j} = \frac{2\alpha_k^2 h_{r,o_k}^2 h_{o_k,u_j}^2 g_r P_t^2}{\sigma_{n_{u_j}}^2}. \tag{18}
$$

Then according to the (13) and related analysis in Section III-B, we can derive the CDF of γ_{r,u_j} as

$$
\begin{aligned}
F_{\gamma_{r,u_j}}(\gamma_{th}) &= \frac{1}{2} exp\left(\varepsilon_{r,u_j}\chi_{r,u_j} + 2\varepsilon_{r,u_j}\sigma_X^2 + 2\varepsilon_{r,u_j}^2\sigma_X^2\right) \\
&\times erfc\left(\frac{\chi_{r,u_j} + 2\sigma_X^2 + 4\varepsilon_{r,u_j}\sigma_X^2}{\sqrt{8}\sigma_X}\right) \\
&- \frac{1}{2} erfc\left(\frac{\chi_{r,u_j} + 2\sigma_X^2}{\sqrt{8}\sigma_X}\right),
\end{aligned} \tag{19}
$$

where $\varepsilon_{r,u_j} = \frac{\omega_{zeq}^2}{4\sigma_{\theta_r'}^2\left(l_{r,o_i}+l_{o_i,u_j}\right)^2+16\sigma_{\beta_i}^2 l_{r,o_i}^2}$, and $\chi_{r,u_j} = \frac{1}{2}ln\frac{\gamma_{th}}{2} + ln\frac{\sigma_{n_{u_j}}}{A_0 P_t \alpha_k g_r h_{l_{r,u_j}}}$. Substituting (16) and (19) into (14), we can obtain the outage probability of the user j 's received signal $P_{out}(\gamma_{th})$.

B. Asymptotic Analysis

In this work, the asymptotic performance expressions can be derived based on the analytical technique in [19]. According to [19], we can perform Taylor expansion on P_{OUT} and remove the higher-order terms of $\frac{1}{\overline{\gamma}}$, so as to obtain the asymptotic outage probability expression under high SNR. Then the aymptotic outage probability can be estimated as (20).

As conditional BER of coherent modulation scheme is $P_e(\tau) = \eta Q(\sqrt{\overline{\gamma}\zeta\tau})$, we can obtain the asymptotic average BER as (21). From (20) and (21), we can observe that the performance of our cascaded system is dominated by the worst link, which depends on the parameters of the two links.

$$P_{out}^{\infty}(\gamma_{th}) \approx \frac{1}{2}\left(\frac{\sigma_{n_r}}{\sqrt{2}A_o P_t h_{l_{s,r}}}\right)^{\varepsilon_{s,r}} e^{2\varepsilon_{s,r}\sigma_X^2+2\varepsilon_{s,r}^2\sigma_X^2}\cdot\gamma_{th}^{\frac{\varepsilon_{s,r}}{2}} + \frac{1}{2}\left(\frac{\sigma_{n_{u_j}}}{\sqrt{2}A_o P_t \alpha_k g_r h_{l_{r,u_j}}}\right)^{\varepsilon_{r,u_j}} e^{2\varepsilon_{r,u_j}\sigma_X^2+2\varepsilon_{r,u_j}^2\sigma_X^2}\cdot\gamma_{th}^{\frac{\varepsilon_{r,u_j}}{2}}. \tag{20}$$

$$\begin{aligned} P_e^{\infty} = \int_0^{\infty} \eta Q(\sqrt{\overline{\gamma}\zeta\gamma}) f_\gamma(\gamma) d\gamma &\approx 2^{\frac{\varepsilon_{s,r}}{2}-2}\frac{\eta\Gamma\left(\frac{\varepsilon_{s,r}+1}{2}\right)}{\sqrt{\pi}}\left(\frac{\sigma_{n_r}}{\sqrt{2\zeta}A_o P_t h_{l_{s,r}}}\right)^{\varepsilon_{s,r}}\cdot e^{2\varepsilon_{s,r}\sigma_X^2-2\varepsilon_{s,r}^2\sigma_X^2} \\ &+ 2^{\frac{\varepsilon_{r,u_j}}{2}-2}\frac{\eta\Gamma\left(\frac{\varepsilon_{r,u_j}+1}{2}\right)}{\sqrt{\pi}}\left(\frac{\sigma_{n_{u_j}}}{\sqrt{2\zeta}A_o P_t \alpha_k g_r h_{l_{r,u_j}}}\right)^{\varepsilon_{r,u_j}}\cdot e^{2\varepsilon_{r,u_j}\sigma_X^2-2\varepsilon_{r,u_j}^2\sigma_X^2}. \end{aligned} \tag{21}$$

V. NUMERICAL RESULTS

We compare analytical results and simulation results in this section. The simulation in this paper is based on the practical physical modeling. In this system, the source uses a laser with a wavelength of 1550 nm, and sends an optical signal to the relay. Then, after collimating and amplifying the optical signal, the relay forwards it to OIRS. The optical signal is reflected by the OIRS to reach the user. We have added independent jitter random variables to the direction vector of the optical beam and the normal vector of the OIRS surface. At the transmitting end, we simulated 10^8 independent signals, and used Monte Carlo method at the receiving end to count the outage probability and BER. The parameters in the systems are presented in Table I. Comparing the curves with different σ_{θ_t} and σ_β, we can observe that the variety of pointing error brings about a large impact on performance. Compared with pointing error jitter at OIRS, pointing error jitter at the transmitter has a greater impact on system performance. Comparing the curves with different σ_R, we can observe that changes in atmospheric turbulence parameters have relatively little impact on system performance, which indicates that the impact of pointing error in FSO links dominates. Comparing the curves with different link distance L, we can observe that as the channel length increases, the system performance deteriorates, which is due to the joint effect of channel fading parameters such as diffusion angle and pointing error. Therefore, the secondary collimation of the optical signal by the optical relay in this system is very necessary.

TABLE I: SYSTEM SETTINGS

Parameters	value
Optical wavelength (λ)	1550 nm
Noise variance at relay ($\sigma_{n_r}^2$)	10^{-6} W
Noise variance at receiver ($\sigma_{n_{u_j}}^2$)	10^{-6} W
Optical signal gain of the relay (g_r)	1.5
Attenuation coefficient introduced by OIRS α	0.9
Receiver diameter at the relay ($2a_1$)	20 cm
Receiver diameter at the user ($2a_2$)	30 cm

VI. CONCLUSION

In this work, we propose a hybrid relay and OIRS-aided distributed FSO system, and perform mathematical modeling on it. The closed-form solutions of the system's performance have been derived. According to theoretical analysis and simulation results, we can observe that the joint work of relay and OIRS not only improves system performance, but also introduces certain channel fading and signal loss. In future work, we need to find ways to reduce these signal losses, so as to further optimize the system as a whole.

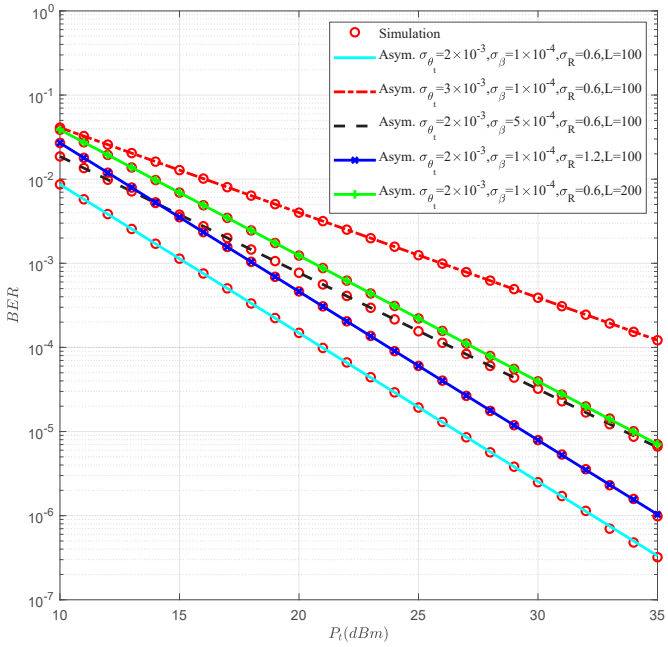

Fig. 2: The asymptotic BERs and the simulated BERs for the hybrid relay and OIRS-aided distributed FSO system with different parameters, the asymptotic results are obtained from (21).

REFERENCES

[1] T. Q. Wang, R. J. Green, and J. Armstrong, "Mimo optical wireless communications using aco-ofdm and a prism-array receiver," *IEEE J. Sel. Areas Commun.*, vol. 33, no. 9, pp. 1959–1971, 2015.

[2] S. Nath, S. Sengar, S. K. Shrivastava, and S. P. Singh, "Impact of atmospheric turbulence, pointing error, and traffic pattern on the performance of cognitive hybrid fso/rf system," *IEEE Trans. Cogn. Commun. Netw.*, vol. 5, no. 4, pp. 1194–1207, 2019.

[3] A. A. Farid and S. Hranilovic, "Outage capacity optimization for free-space optical links with pointing errors," *J. Lightw. Tech.*, vol. 25, no. 7, pp. 1702–1710, 2007.

[4] X. Huang, X. Xie, J. Song, T. Duan, H. Hu, X. Xu, and Y. Su, "Performance comparison of all-optical amplify-and-forward relaying fso communication systems with ook and dpsk modulations," *IEEE Photon. J.*, vol. 10, no. 4, pp. 1–11, 2018.
[5] W. Liu, J. Ding, J. Zheng, X. Chen, and C.-L. I, "Relay-assisted technology in optical wireless communications: A survey," *IEEE Access*, vol. 8, pp. 194 384–194 409, 2020.
[6] E. Zedini and M.-S. Alouini, "Multihop relaying over im/dd fso systems with pointing errors," *J. Lightw. Techn.*, vol. 33, no. 23, pp. 5007–5015, 2015.
[7] S. Sun, T. Wang, F. Yang, J. Song, and Z. Han, "Intelligent reflecting surface-aided visible light communications: Potentials and challenges," *IEEE Vehi. Techn. Mag.*, vol. 17, no. 1, pp. 47–56, 2022.
[8] W. Pang, P. Wang, M. Han, S. Li, P. Yang, G. Li, and L. Guo, "Optical intelligent reflecting surface for mixed dual-hop fso and beamforming-based rf system in c-ran," *IEEE Trans. Wireless Commun.*, pp. 1–1, 2022.
[9] S. Sun, F. Yang, and J. Song, "Sum rate maximization for intelligent reflecting surface-aided visible light communications," *IEEE Commun. Lett.*, vol. 25, no. 11, pp. 3619–3623, 2021.
[10] H. Wang, Z. Zhang, B. Zhu, J. Dang, L. Wu, L. Wang, K. Zhang, Y. Zhang, and G. Y. Li, "Performance analysis of multi-branch reconfigurable intelligent surfaces-assisted optical wireless communication system in environment with obstacles," *IEEE Trans. Vehi. Tech.*, vol. 70, no. 10, pp. 9986–10 001, 2021.
[11] C. Sun, J. Wang, X. Gao, and Z. Ding, "Networked optical massive mimo communications," *IEEE Trans Wireless Commun.*, vol. 19, no. 8, pp. 5575–5588, 2020.
[12] R. Papannareddy and A. Weiner, "Performance comparison of coherent ultrashort light pulse and incoherent broad-band cdma systems," *IEEE Photon. Techn. Lett.*, vol. 11, no. 12, pp. 1683–1685, 1999.
[13] A. Memedi and F. Dressler, "Vehicular visible light communications: A survey," *IEEE Commun. Surveys and Tut.*, vol. 23, no. 1, pp. 161–181, 2021.
[14] V. Jamali, H. Ajam, M. Najafi, B. Schmauss, R. Schober, and H. V. Poor, "Intelligent reflecting surface assisted free-space optical communications," *IEEE Commun. Mag.*, vol. 59, no. 10, pp. 57–63, 2021.
[15] M. Najafi, B. Schmauss, and R. Schober, "Intelligent reflecting surfaces for free space optical communication systems," *IEEE Trans. Commun.*, vol. 69, no. 9, pp. 6134–6151, 2021.
[16] M. Najafi and R. Schober, "Intelligent reflecting surfaces for free space optical communications," in *Proc. IEEE Global Commun. Conf.*, 2019, pp. 1–7.
[17] M. Ijaz, Z. Ghassemlooy, J. Perez, V. Brazda, and O. Fiser, "Enhancing the atmospheric visibility and fog attenuation using a controlled fso channel," *IEEE Photon. Technol. Lett.*, vol. 25, no. 13, pp. 1262–1265, 2013.
[18] A. Prokes, O. Wilfert, and J. Petrzela, "Comparison of atmospheric losses in 850 nm and 1550 nm optical windows," in *Proc. IEEE Reg. Int. Conf. Comput. Technol. Electr. Electron. Eng.*, 2010, pp. 310–313.
[19] Z. Wang and G. B. Giannakis, "A simple and general parameterization quantifying performance in fading channels," *IEEE Trans. Commun.*, vol. 51, no. 8, pp. 1389–1398, Aug. 2003.